BIOCHEMISTRY
including biophysical chemistry & molecular biology
Accelerated Publication

Biochemistry **2010,** *49,* 3517–3524 3517
DOI: 10.1021/bi100318v

X-ray Structure of KijD3, a Key Enzyme Involved in the Biosynthesis of D-Kijanose[†,‡]

Nathan A. Bruender, James B. Thoden, and Hazel M. Holden*

Department of Biochemistry, University of Wisconsin, Madison, Wisconsin 53706

Received March 3, 2010

ABSTRACT: D-Kijanose is an unusual nitrosugar found attached to the antibiotic kijanimicin. Ten enzymes are required for its production in *Actinomadura kijaniata*, a soil-dwelling actinomycete. The focus of this investigation is on the protein encoded by the *kijd3* gene and hereafter referred to as KijD3. On the basis of amino acid sequence analyses, KijD3 has been proposed to be an FAD-dependent oxidoreductase, which catalyzes the sixth step in D-kijanose biosynthesis by converting dTDP-3-amino-2,3,6-trideoxy-4-keto-3-methyl-D-glucose into its C-3′ nitro derivative. This putative activity, however, has never been demonstrated in vivo or in vitro. Here we report the first structural study of this enzyme. For our investigation, crystals of KijD3 were grown in the presence of dTDP, and the structure was solved to 2.05-Å resolution. The enzyme is a tetramer with each subunit folding into three distinct regions: a five α-helical bundle, an eight-stranded β-sheet, and a second five α-helical bundle. The dTDP moiety is anchored to the protein via the side chains of Glu 113, Gln 254, and Arg 330. The overall fold of KijD3 places it into the well-characterized fatty acyl-CoA dehydrogenase superfamily. There is a decided cleft in each subunit with the appropriate dimensions to accommodate a dTDP-linked sugar. Strikingly, the loop defined by Phe 383 to Ala 388, which projects into the active site, contains two adjacent cis-peptide bonds, Pro 386 and Tyr 387. Activity assays demonstrate that KijD3 requires FAD for activity and that it produces a hydroxylamino product. The molecular architecture of KijD3 described in this report serves as a paradigm for a new family of enzymes that function on dTDP-linked sugar substrates.

The unusual di- and trideoxysugars distributed throughout nature represent an especially intriguing class of carbohydrates (*1*, *2*). They are found, for example, on the lipopolysaccharides of some Gram-negative bacteria (*3*), on the *S*-layers of some Gram-positive and Gram-negative bacteria (*4*), and on extracellular polysaccharides (*5*). They are also found attached to natural products, where they often play key roles in the efficacies of these compounds (*6*−*10*). The widely used chemotherapeutic agent, doxorubicin, for example, contains the sugar daunosamine appended to its aglycone scaffold. Without daunosamine, the therapeutic value of doxorubicin is severely reduced, and it has been demonstrated that modifications to the sugar result in markedly different toxicities and anticancer activities of the drug (*11*−*13*).

Within recent years the less common, though not less biologically important, nitrosugars have attracted research interest (*14*). These hydroxyamino-, nitroso-, and nitro-containing carbohydrates are derived via the oxidation of the corresponding aminosugars. The nitrosugar D-kijanose (Scheme 1), for example, is found on kijanimicin (*15*) a spirotetronate antibiotic produced by *Actinomadura kijaniata* (ATCC 31588). Of medical relevance is the fact that kijanimicin demonstrates a wide range of biological functions, ranging from antibacterial, to antifungal and antitumor activities (*8*). The sugar itself is appended to the pentacyclic core of kijanimicin via the action of a glycosyltransferase that requires D-kijanose to be linked to dTDP[1] (*15*).

The biosynthesis of dTDP-D-kijanose in *A. kijaniata* requires 10 enzymes. The focus of this investigation is on the enzyme encoded by the *kijD3* gene, and hereafter referred to as KijD3 (*15*). It has been postulated to catalyze the oxidation of the C-3′ amino group of dTDP-3-amino-2,3,6-trideoxy-4-keto-3-methyl-D-glucose to the C-3′ nitro derivative as shown in Scheme 1. Homologous proteins of KijD3 have been observed in other organisms that synthesize nitrosugars including RubN8, EvdC, and TcaB10 from the D-rubranitrose, L-evernitrose, and D-tetranitrose biosynthetic pathways, respectively (*16*−*18*). All of these enzymes are thought to require flavin cofactors for activity, and recently both RubN8 and EvdC have been shown to utilize FAD in the conversion of their aminosugar substrates to nitrososugar products (*19*). Until this report, however, there were no known three-dimensional structures for any of these enzymes, and no detailed kinetic analyses are yet available.

Here we describe the first three-dimensional structure of KijD3 determined to a nominal resolution of 2.05-Å. For this analysis, the enzyme was complexed with dTDP. Our investigation shows that each subunit of the tetrameric enzyme adopts a fold characteristic for enzymes belonging the fatty acyl-CoA dehydrogenase superfamily (*20*, *21*). Details concerning the molecular architecture of the KijD3 active site are presented.

MATERIALS AND METHODS

Cloning, Expression, and Purification. A. kijaniata (ATCC 31588) was obtained from the American Type Culture Collection, and genomic DNA was isolated according to standard

[†]This research was supported in part by an NSF Grant (MCB-0849274 to H.M.H.).

[‡]X-ray coordinates have been deposited in the Research Collaboratory for Structural Bioinformatics, Rutgers University, New Brunswick, N. J. (accession no. 3M9V).

*To whom correspondence should be addressed. E-mail: Hazel_Holden@biochem.wisc.edu. Fax: 608-262-1319. Phone: 608-262-4988.

[1]Abbreviations: DTT, dithiothreitol; ESI, electrospray ionization; FAD, flavin adenine dinucleotide; HEPES, 4-(2-hydroxyethyl)-1-piperazine-ethane sulfonic acid; HPLC, high performance liquid chromatography; IPTG, isopropyl-β-D-thiogalactopyranoside; LB, Luria−Bertani; Ni-NTA, nickel-nitrilotriacetic acid; PCR, polymerase chain reaction; dTDP, deoxythymidine diphosphate; TEV, tobacco etch virus.

Published on Web 03/24/2010

Scheme 1

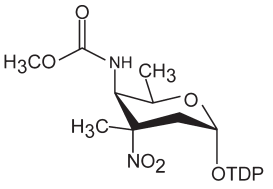

dTDP- kijanose

[2,3,4,6-tetradeoxy-4-(methylcarbamyl)-3-*C*-methyl-3-nitro-D-*xylo*-hexopyranose]

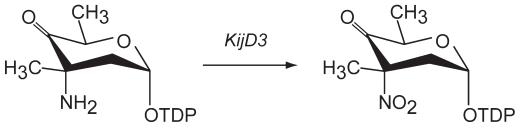

protocols. The *kijd3* gene was PCR-amplified from genomic DNA using the forward primer 5′-AAAA*CATATG*CCCCCAT-GGACGGCACG-3′ and the reverse primer 5′-AAAA*CTC-GAG*TCACCGTGACGTGGGTGTAGGA-3′, which added *Nde*I and *Xho*I cloning sites, respectively. The purified PCR product was A-tailed and ligated into a pGEM-T (Promega) vector for blue-white screening and sequencing. A *kijd3*-pGEM-T vector construct of the correct sequence was then digested with *Nde*I and *Xho*I, and the gene was ligated into a pET28JT vector (*22*) for production of protein with a TEV protease cleavable N-terminal hexahistidine tag.

The *kijd3*-pET28JT plasmid was used to transform either BL-21(DE3) or HMS 174 *Escherichia coli* cells (Novagen). The cultures were grown in LB medium supplemented with kanamycin at 37 °C with shaking until optical densities of ~0.6, measured at 600 nm, were reached. The flasks were then cooled to 16 °C and induced with 1 mM IPTG. The cells were allowed to express protein at 16 °C for 18 h. KijD3 was purified at 4 °C following standard procedures using Ni-NTA resin (Qiagen). Half of the purified protein was incubated in the presence of 1 mM DTT and TEV protease in a 50:1 (KijD3:TEV protease) molar ratio at room temperature for 36 h. The TEV protease was subsequently removed via Ni-NTA column chromatography. Both preparations of KijD3 (TEV-cleaved and His-tagged) were dialyzed against 20 mM HEPES (pH 7.5) and 100 mM NaCl. The protein preparations were concentrated to approximately 20 mg/mL using an extinction coefficient of 0.92 $(mg/mL)^{-1}$ cm^{-1} at 280 nm and were subsequently flash frozen in liquid nitrogen.

Crystallization of KijD3. Crystallization conditions were initially surveyed for both protein constructs by the hanging drop method of vapor diffusion using a sparse matrix screen developed in the laboratory. The apo-forms of the two protein constructs as well as the binary complexes with either 10 mM FAD or 20 mM dTDP-phenol were subjected to crystallization trials. All protein concentrations were at 15 mg/mL. Diffraction quality crystals of the N-terminal His-tagged enzyme were grown by mixing in a 1:1 ratio the enzyme incubated with 10 mM FAD and 23−26% (w/v) pentaerythritol propoxylate (5/4) at pH 5.5. These crystals belonged to the space group *I*222 with one monomer per asymmetric unit and the following unit cell dimensions: a = 73.3 Å, b = 82.7 Å, and c = 153.1 Å. Crystals of the TEV-cleaved enzyme were grown by mixing in a 1:1 ratio the enzyme incubated with 20 mM dTDP-phenol and 1.3 M - 1.6 M ammonium sulfate at pH 5.5. These crystals also belonged to the space group *I*222 with one monomer per asymmetric unit and the following unit cell dimensions: a = 72.9 Å, b = 82.5 Å, and c = 153.2 Å.

Structural Analysis of KijD3. All X-ray data sets were measured at 4 °C with a Bruker HI-STAR area detector system. The X-ray source was Cu Kα radiation from a Rigaku RU200 X-ray generator equipped with Supper mirrors and operated at 50 kV and 90 mA. These X-ray data were processed with SAINT version 7.06A (Bruker AXS Inc.) and internally scaled with SADABS version 2005/1 (Bruker AXS Inc.). Relevant X-ray data collection statistics are presented in Table 1.

An initial structure of the N-terminal tagged enzyme was solved with two heavy atom derivatives, which were prepared by soaking the crystals in either 8 mM potassium gold(I) cyanide or 28 mM trimethyl lead acetate for 3 days or 5 days, respectively. Prior to X-ray data collection, these crystals were stabilized by transfer into a 30% pentaerythritol propoxylate (5/4) solution (pH 7.0) containing 10 mM FAD and 100 mM NaCl. Three gold and five lead binding sites were identified with SOLVE giving an overall figure of merit of 0.39 to 2.8 Å (*23*, *24*). Solvent flattening with RESOLVE generated an interpretable electron density map (*24*, *25*). A preliminary model was constructed using COOT (*26*). In the original model, there was no interpretable electron density corresponding to FAD suggesting that it did not bind tightly.

This preliminary model was subsequently utilized as a search probe for determining the structure of the enzyme-dTDP-phenol complex via molecular replacement with the software package PHASER (*27*). Refinement with Refmac using maximum likelihood reduced the R_{factor} to 17.1% for all measured X-ray data from 50 to 2.05 Å resolution (*28*). Relevant refinement statistics are presented in Table 2.

Production of dTDP-3-amino-2,3,6-trideoxy-4-keto-3-methyl-D-glucose. The KijD3 substrate was enzymatically synthesized using dTDP-D-glucose as the starting material. Enzymes required for the synthesis were a 4,6-dehydratase (RmlB), a 2,3-dehydratase (EvaA), a 3-aminotransferase (TcaB8), and a *C*-3-methyltransferase (KijD1). All of the required enzymes were purified in the laboratory. A typical reaction contained the following: 50 mM HEPES (pH 7.5), 100 mM NaCl, 10 mM $MgCl_2$, 20% glycerol, 20 mM L-glutamate, 2 mM *S*-adenosylmethionine, 10 mg/mL dTDP-D-glucose, 0.8 mg/mL of RmlB, 0.25 mg/mL of EvaA, and 3 mg/mL each of TcaB8 and KijD1. The reaction was allowed to proceed at 20 °C for 16 h. All enzymes were removed with a 30-kDa cutoff Centriprep concentrator, and the filtrate was diluted 1:7.5 with water. The sugar was purified via an AKTA Purifier HPLC (GE Healthcare) equipped with a 6 mL Resource Q anion exchange column (GE Healthcare) using a 78 mL linear gradient from 0 to 130 mM ammonium acetate at pH 4.0. The desired product peak was identified by ESI mass spectrometry (Mass Spectrometry/Proteomics Facility at the University of Wisconsin-Madison). Fractions containing the amino sugar were pooled and diluted 1:4 with water, the pH was adjusted to 8.0, and the sugar was further purified via the 6 mL Resource Q column using a 120 mL linear gradient from 0 to 250 mM of ammonium bicarbonate at pH 8.5. Fractions of the amino sugar were pooled and lyophilized until all traces of the buffer were removed. Typical yields of this compound were ~5% based on the starting amount of dTDP-glucose.

Measurement of Enzymatic Activity. Enzymatic activity was determined via HPLC. For each reaction, 1 mg of KijD3 was added to a 1 mL solution containing 50 mM HEPES (pH 7.5),

Table 1: X-ray Data Collection Statistics

	enzyme complexed with FAD	gold heavy atom derivative	lead heavy atom derivative	enzyme complexed with dTDP-phenol
resolution limits	50.0−2.5 (2.6−2.5)[b]	50−2.8 (2.9−2.8)[b]	50.0−2.8 (2.9−2.8)[b]	50.0−2.05 (2.15−2.05)[b]
number of independent reflections	15441 (1258)	11265 (1019)	11522 (996)	27721 (2824)
completeness (%)	90.7 (69.3)	95.4 (85.1)	95.5 (80.5)	94.2 (80.7)
redundancy	2.9 (1.7)	3.1 (1.9)	2.9 (1.6)	3.5 (1.5)
avg I/avg $\sigma(I)$	7.4 (3.1)	7.2 (2.6)	6.8 (2.3)	10.7 (3.5)
R_{sym} (%)[a]	11.2 (25.9)	12.5 (30.5)	12.5 (31.1)	8.1 (19.6)

[a] $R_{sym} = (\sum| I - \bar{I}|/ \sum I) \times 100$. [b] Statistics for the highest resolution bin.

Table 2: Refinement Statistics

	enzyme complexed with dTDP-phenol
resolution limits (Å)	50.0−2.05
R[a]-factor (overall)%/no. reflections	17.1/27721
R-factor (working)%/no. reflections	16.8/26300
R-factor (free)%/no. reflections	22.1/1420
number of protein atoms	2904[b]
number of heteroatoms	133[c]
average B values	
protein atoms (Å^2)	27.6
ligand (Å^2)	44.3
solvent (Å^2)	35.9
weighted rms deviations from ideality	
bond lengths (Å)	0.009
bond angles (°)	2.0
planar groups (Å)	0.008
Ramachandran regions (%)[d]	
most favored	93.7
additionally allowed	6.0
generously allowed	0.3
disallowed	0.0

[a] R-factor $= (\Sigma|F_o - F_c|/\Sigma|F_o|) \times 100$ where F_o is the observed structure-factor amplitude and F_c is the calculated structure-factor amplitude. [b] These include multiple conformations for Ser 38, Thr 51, Ser 164, and Arg 347. [c] Heteroatoms include a dTDP molecule and 108 waters. [d] Distribution of Ramachandran angles according to PROCHECK (*32*).

100 mM NaCl, 0.5 mM dTDP-3-amino-2,3,6-trideoxy-4-keto-3-methyl-D-glucose, 30 μM FAD, 1 U/mL catalase, 1 U/mL superoxide dismutase, 5 mM NADPH, and 0.001 mg/mL of the flavin reductase, Fre, from *E. coli*. The reaction was allowed to proceed at 30 °C, and aliquots were taken to monitor the progress of the reaction as a function of time. For each aliquot, the enzyme was removed via filtration, and the filtrate was diluted 1:9 with water. The various diluted reaction mixtures were analyzed via an AKTA Purifier HPLC (GE Healthcare) equipped with a 1 mL Resource Q anion exchange column (GE Healthcare) and using a 20 mL linear gradient from 30 to 250 mM ammonium bicarbonate at pH 8.5. The desired product peak was identified by ESI mass spectrometry.

RESULTS AND DISCUSSION

Activity Assays. The KijD3 homologues, RubN8 from *Streptomyces achromogenes* and EvdC from *Micromonospora carbonacea*, were recently characterized as nitrososynthases based on activity assays (*19*). Both of these enzymes converted the substrate analogue L-dTDP-*epi*-vancosamine to a nitroso sugar product in a two-step process, with the first step leading to the formation of a hydroxylamino intermediate. Interestingly, formation of a nitro-containing product, however, was never observed (*19*). Note that unlike the KijD3 substrate which has an activating keto group at the sugar C-4′, the substrate analogue used in the analyses of RubN8 and EvdC contained a C-4′ hydroxyl moiety. On the basis of the above-described activity assays, it was proposed that RubN8 and EvdC function as nitroso- rather than nitrosynthases and that the final oxidation of the nitroso to the nitrosugar occurs via a photochemical process. Such a photochemical reaction was previously shown to be operative in the formation of rubranitrose, a nitrosugar found in the antibiotic rubradirin (*29*).

Although KijD3 was annotated as an FAD-dependent oxidoreductase, its actual activity was never tested (*15*). Given the amino acid sequence homology between KijD3 and RubN8 (62% identity) or EvdC (65% identity), however, we suspected that KijD3 might function as a nitrososynthase as well. To test this hypothesis, reactions were set up as described in the Materials and Methods. At $t = 0$ min, the HPLC chromatogram showed a broad peak with a retention time of 7.2 min (Figure 1a). ESI mass spectrometry demonstrated that this peak corresponded to the substrate, dTDP-3-amino-2,3,6-trideoxy-4-keto-3-methyl-D-glucose with a $m/z = 542$ (Figure 1b). Over time, this region of the elution profile underwent a distinct sharpening suggesting the emergence of a new molecular species, as indicated by the spectra taken at 90 and 360 min (Figure 1a). The HPLC chromatograms indicated that catalysis was occurring because when either KijD3 or the *E. coli* flavin reductase or both were excluded from the reaction, the peak corresponding to dTDP-3-amino-2,3,6-trideoxy-4-keto-3-methyl-D-glucose remained unchanged.

The peaks corresponding to 2 and 6 h reaction times were purified and subjected to mass spectrometry. The mass spec for the HPLC peak following a 2 h reaction time demonstrated a predominant peak with a $m/z = 558$, which corresponds to a hydroxylamino sugar (Figure 1c). The mass spec for the HPLC peak following a 6 h reaction time again showed a peak with a $m/z = 558$ (Figure 1d). There was, however, a more predominant peak at $m/z = 527$, which may represent the decomposition of a nitrosugar to dTDP-2,3,6-trideoxy-4-keto-3-methyl-D-glucose. While we were never able to directly observe the formation of the nitrosugar in our experiments, there is the possibility that the keto group at the sugar C-4′ enhanced its decomposition. Regardless, these data indicate that the KijD3 sample employed for the structural studies described here is enzymatically active. More detailed kinetic analyses are presently underway.

Overall Molecular Architecture. The structure of KijD3 was solved to 2.05-Å resolution and refined to an R_{factor} of 17.1% for all measured reflections. For the most part, the quality of the electron density was unambiguous with the exception of the following missing residues: Met 1 - Asp 9, Thr 188 - Asp 189,

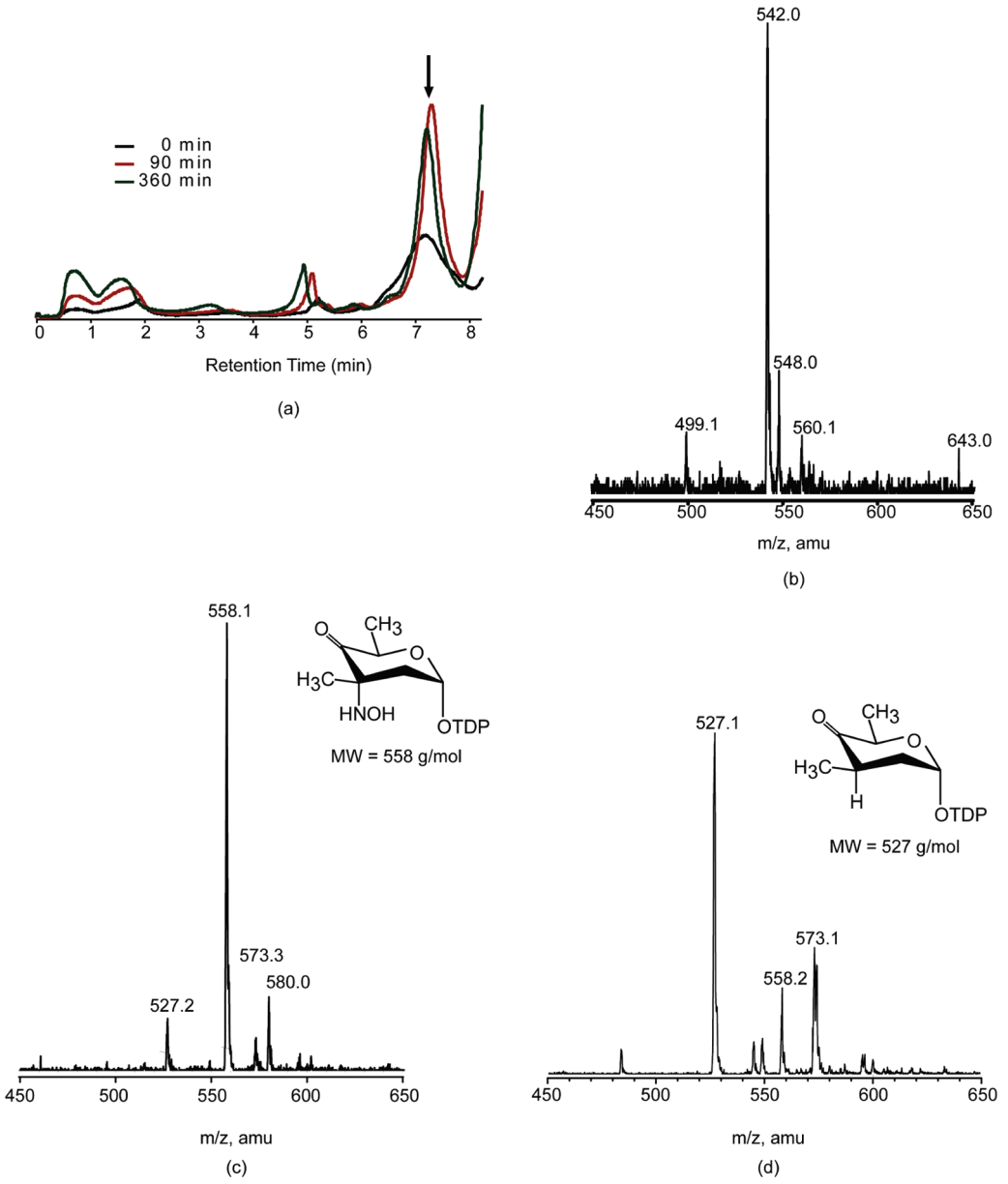

FIGURE 1: Shown in (a) is the HPLC chromatogram overlay of the 0 min, 90 min, and 360 min time points for the KijD3 activity assay. The arrow indicates the peak of interest. The mass spectrum presented in (b) is that of the HPLC peak purified after a reaction time of 0 h. The peak at m/z = 542 corresponds to KijD3 substrate (Scheme 1). The mass spectrum presented in (c) is that of the HPLC peak purified after a reaction time of 2 h. The peak at m/z = 558 corresponds to the indicated hydroxylamine sugar. The mass spectrum presented in (d) is that of the HPLC peak purified after a reaction time of 6 h. The peak at m/z = 558 corresponds to the hydroxylamino sugar, whereas that at m/z = 527 may correspond to the breakdown product, dTDP-2,3,6-trideoxy-4-keto-3-methyl-D-glucose.

Val 243 - Gly 244, and Glu 404 - Arg 437. Representative electron density corresponding to the bound dTDP ligand is presented in Figure 2a. Both Pro 386 and Tyr 387 adopt cis-peptide conformations, which in tandem is highly unusual (Figure 2b). This cis-peptide rich turn is positioned on one side of the active site as discussed below.

The KijD3 tetramer packed in the crystalline lattice along three crystallographic dyads thereby resulting in one subunit per asymmetric unit. A ribbon representation of the tetramer, with overall dimensions of ~86 × 88 × 84 Å, is displayed in Figure 3a. The tetramer can be aptly described as a dimer of dimers with the two active sites in each dimer separated by ~50 Å. The buried surface area per subunit is ~3100 Å^2. Most of the subunit/subunit interactions are provided by the polypeptide chain from Arg 336 - Leu 401, which folds into three α-helical regions. There are two additional loops, defined by Ser 10 - Tyr 15 and Asp 213 - Met 217, which project toward the subunit:subunit interface. Shown in Figure 3b is a ribbon representation of an individual subunit with overall dimensions of ~73 × 51 × 50 Å. The architecture of the subunit can be described in terms of three distinct regions. The first, formed by Pro 20 - Ala 134, adopts a five α-helical bundle architecture. Following this region, the polypeptide chain folds into an eight-stranded β-sheet barrel (Val 138 - Asn 247). The β-barrels in the tetramer extend away from the subunit:subunit interfaces. The final region of the subunit (Asp 248 - Ile 403) also contains a five α-helical bundle, and it provides most of the contacts between monomers in the tetramer.

For this X-ray analysis, the protein was crystallized in the presence of dTDP-phenol. The electron density map clearly revealed only the presence of the nucleotide, however. Either the aromatic ring was disordered or more likely the dTDP-phenol solution used for this study contained dTDP, which preferentially

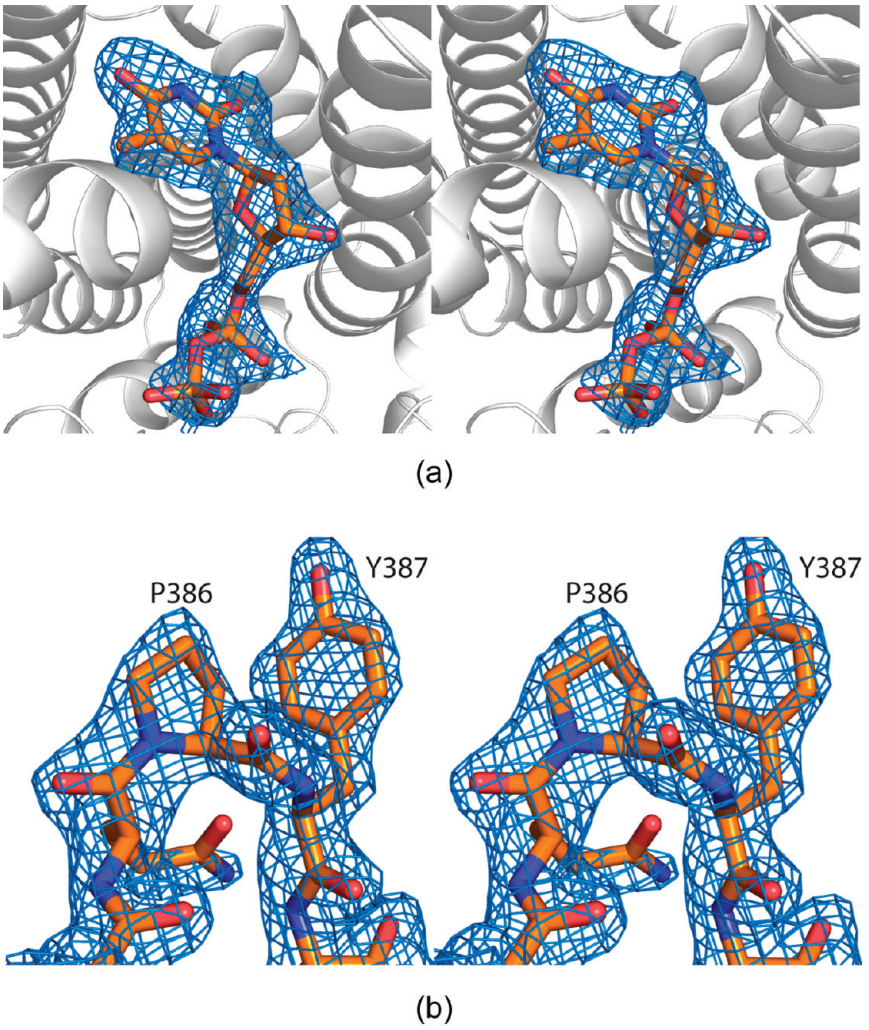

FIGURE 2: Representative electron densities. Shown in (a) is the observed electron density for the bound dTDP ligand. The electron density presented in (b) corresponds to the loop defined by Phe 383 - Ala 388. Both Pro 386 and Tyr 387 adopt cis peptide conformations. The electron densities were calculated with coefficients of the form ($F_o - F_c$), where F_o was the native structure factor amplitude and F_c was the calculated structure factor amplitude with atoms corresponding to either the nucleotide (a) or the polypeptide chain (b) excluded from the calculations. The maps were contoured at 2.5σ and 3.0σ, respectively.

bound to the enzyme. A close-up view of the dTDP binding pocket is displayed in Figure 3c. The thymine base is anchored to the protein via the guanidinium group of Arg 330 and a water molecule, whereas the ribose 3-hydroxyl group hydrogen bonds with the carboxylate of Glu 113. The α- and β-phosphoryl groups of the nucleotide interact with Ser 257 and Gln 254, respectively.

A structural search with the software package SSM (*30*) reveals that the molecular architecture of KijD3 is exceedingly similar to that observed for members of the fatty acyl-CoA dehydrogenase superfamily, despite relatively low amino acid sequence homologies ranging from 17 to 26%. A superposition of KijD3 onto the structure of isobutyryl-CoA dehydrogenase (*31*) is presented in Figure 4a. Whereas these two proteins demonstrate an amino acid sequence homology of only 21%, 324 of their α-carbons superimpose with a root-mean-square deviation of 2.0 Å. Given the close structural correspondence between these two enzymes, it is reasonable to conclude that the observed binding position of FAD to isobutyryl-CoA dehydrogenase represents an excellent mimic for flavin-binding to KijD3.

A surface representation of one monomer of KijD3 is displayed in Figure 4b, and as can be seen there is a decided crevice separating the two lobes of the molecule. This cleft has the appropriate dimensions to accommodate a nucleotide-linked sugar. In light of this, and given the location of FAD binding to isobutyryl-CoA dehydrogenase and dTDP binding to KijD3, a model of the KijD3 active site with bound FAD and dTDP-3-amino-2,3,6-trideoxy-4-keto-3-methyl-D-glucose was constructed (Figure 4c). This model predicts that the flavin ring of FAD, when bound to KijD3, is surrounded by the side chains of Leu 98, Met 102, Lys 144, Leu 169, and Met 384. The model also predicts that the hexose moiety of the dTDP-linked sugar binds with its C-3′ methyl group pointing toward the side chain of Ile 143. This side chain forms the only hydrophobic patch in this otherwise reasonably hydrophilic active site (Figure 4c). The opposite side of the hexose abuts the "cis peptide rich" loop defined by Phe 383 - Ala 388 and containing cis-Pro 386 and cis-Tyr 387. It is possible that the polypeptide chain between Thr 188 - Asp 189 and Val 243 - Gly 244 becomes ordered upon dTDP-sugar binding.

At present, there are little published data regarding the catalytic mechanism of KijD3. As discussed above, however, a study on the homologous proteins EvdC and RubN8 suggests that the reaction mechanism of these enzymes proceeds through a process whereby $FADH_2$ reacts with molecular oxygen to form a flavin 4a-hydroperoxide (*19*). In our predicted model, the C-3′ amino group of the substrate is

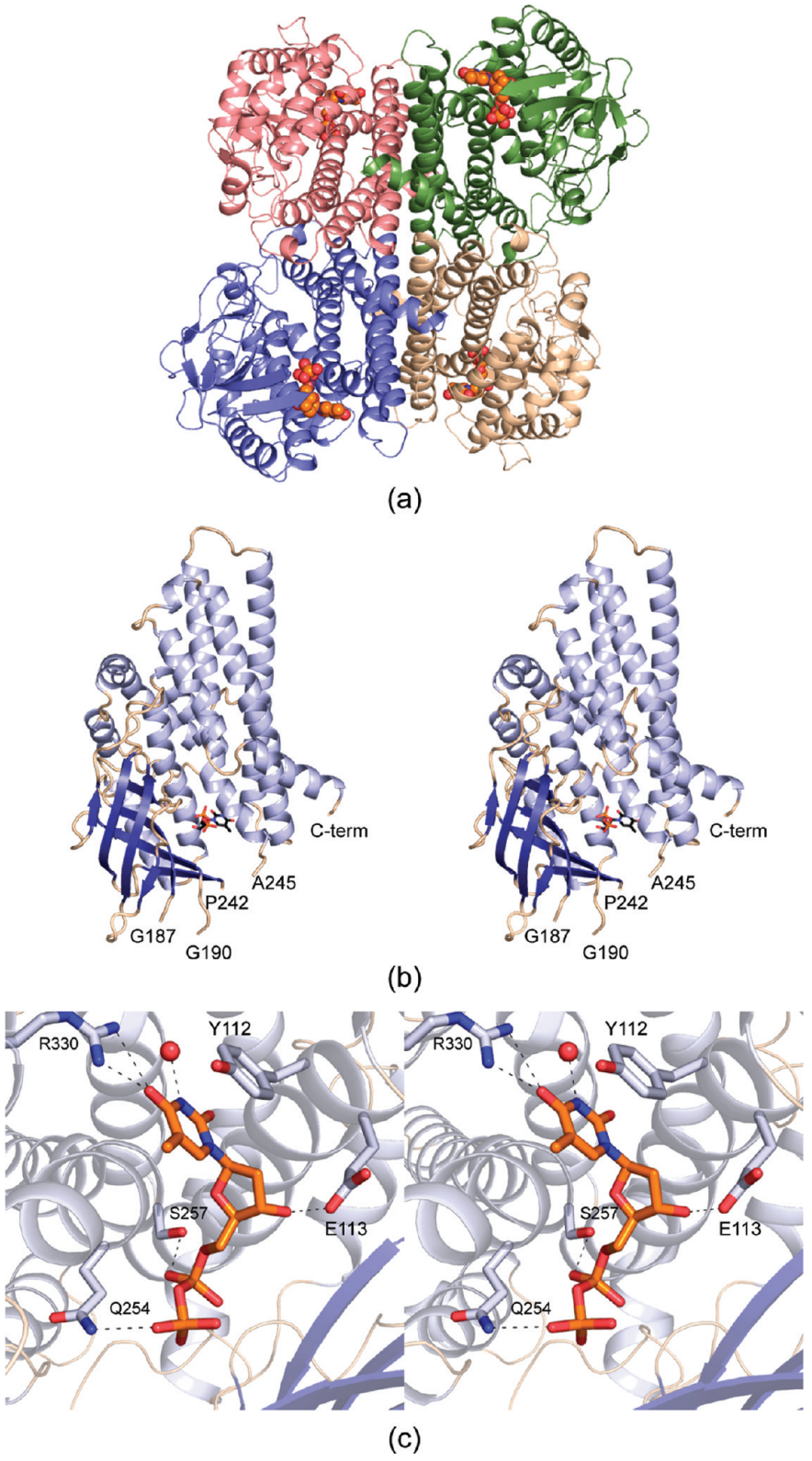

FIGURE 3: The structure of KijD3. A ribbon drawing of the tetramer is presented in (a) with the bound dTDP ligands depicted in space-filling representations. A stereoview of one subunit of KijD3 is shown in (b) with the β-barrel highlighted in darker blue and the nucleotide drawn in a stick representation. Those amino acid residues (or solvent) that are involved in anchoring the nucleotide to the protein are displayed in (c). The water molecule is depicted as a red sphere, and the dashed lines indicate possible hydrogen bonding interactions.

located ~7 Å from the flavin 4a carbon. This would be about the expected distance given that the length of the oxygen-flavin 4a carbon bond is ~1.4 Å and the length of oxygen:oxygen single bond is ~1.5 Å. According to the mechanism proposed by Hu et al., there is an active site acid that protonates the flavin 4a-hydroperoxide species (*19*). Particularly striking in our model is the lack of any potential catalytic acids within the active site pocket except for His 101, which is conserved among the homologues EvdC and RubN8. In the present model, it is located ~8 Å from the flavin 4a carbon.

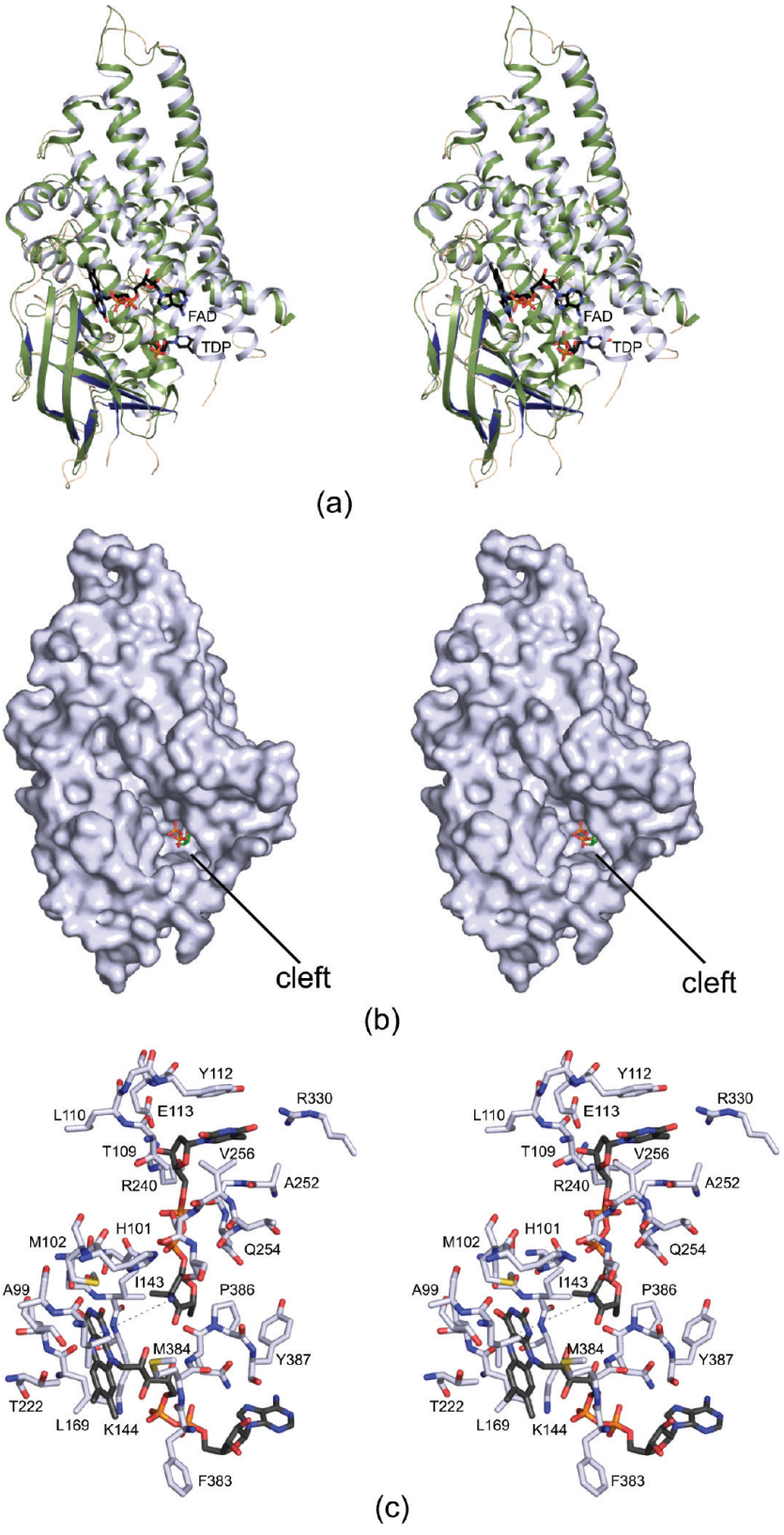

FIGURE 4: Comparison of KijD3 with isobutyryl-CoA dehydrogenase and a possible binding mode for its dTDP-linked sugar substrate. A superposition of the ribbon representations for KijD3 (light and dark blue) and the dehydrogenase (light green) is presented in (a). The binding positions for the FAD and dTDP ligands, shown in stick representations, correspond to those observed in isobutyryl-CoA dehydrogenase and KijD3, respectively. Coordinates for the dehydrogenase (*31*) were obtained from the protein data bank (accession no. 1RX0). A surface representation of the KijD3 subunit is shown in (b). Note the large cleft extending from the pyrophosphoryl group of dTDP to the surface of the subunit. On the basis of the similarities between KijD3 and isobutyryl-CoA dehydrogenase, a model was constructed of the KijD3 active site with bound FAD and dTDP-3-amino-2,3,6-trideoxy-4-keto-3-methyl-D-glucose as shown in (c). The dashed line highlights the distance between the amino group that is ultimately oxidized and the flavin 4a carbon that presumably carries the molecular oxygen required for the reaction. The FAD and dTDP-sugar ligands are highlighted in gray bonds, whereas the protein is displayed in white filled bonds. This figure, as well as figures 2 and 3, were prepared with the software package PyMOL (*33*).

Nitrosugars, although not as common as amino sugars, have been found attached to a variety of natural products including antibacterial, antitumor, antimalaria, anticholesterolemic, antiviral, and antidiabetic agents (*14*). Within recent years, research interest in the proteins required for the production of such nitrosugars has grown, and one of the key enzymes involved in their biosynthesis is KijD3 and its homologues. Given the amino acid sequence similarities between KijD3, EvdC, and RubN8, the three-dimensional architecture of KijD3 described here provides the first molecular scaffold for understanding this fascinating enzyme family.

ACKNOWLEDGMENT

We thank Professor W. W. Cleland for helpful discussions throughout the course of this investigation. We also acknowledge Amanda Carney and Rachel Kubiak for critical reading of the manuscript.

REFERENCES

1. Kennedy, J. F., and White, C. A. (1983) Bioactive Carbohydrates in Chemistry, Biochemistry, and Biology, Ellis Horwood Publishers, Chichester.
2. Russer, F., Bannister, B., Tarpley, W. G., Althaus, I. W., and Zapotocky, B. A. (1988) Patent Cooperation Treaty, W08808707.
3. Schnaitman, C. A., and Klena, J. D. (1993) Genetics of lipopolysaccharide biosynthesis in enteric bacteria. *Microbiol. Rev. 57*, 655–682.
4. Claus, H., Akca, E., Debaerdemaeker, T., Evrard, C., Declercq, J. P., Harris, J. R., Schlott, B., and Konig, H. (2005) Molecular organization of selected prokaryotic *S*-layer proteins. *Can. J. Microbiol. 51*, 731–743.
5. Reeves, P. R. (1994) Bacterial Cell Wall, Elsevier Science, Oxford.
6. Trefzer, A., Salas, J. A., and Bechthold, A. (1999) Genes and enzymes involved in deoxysugar biosynthesis in bacteria. *Nat. Prod. Rep. 16*, 283–299.
7. Johnson, D. A., Liu, H.-w. (1999) Deoxysugars: Occurrence, Genetics, and Mechanisms of Biosynthesis, Vol. *3*, Elsevier, Amsterdam.
8. Waitz, J. A., Horan, A. C., Kalyanpur, M., Lee, B. K., Loebenberg, D., Marquez, J. A., Miller, G., and Patel, M. G. (1981) Kijanimicin (Sch 25663), a novel antibiotic produced by *Actinomadura kijaniata* SCC 1256. Fermentation, isolation, characterization and biological properties. *J. Antibiot.* (*Tokyo*) *34*, 1101–1106.
9. Chen, S. C., and Sorrell, T. C. (2007) Antifungal agents. *Med. J. Aust. 187*, 404–409.
10. Minotti, G., Menna, P., Salvatorelli, E., Cairo, G., and Gianni, L. (2004) Anthracyclines: molecular advances and pharmacologic developments in antitumor activity and cardiotoxicity. *Pharmacol. Rev. 56*, 185–229.
11. Arcamone, F. (1981) Doxorubicin Anticancer Antibiotics, Academic Press, New York, NY.
12. Capranico, G., Supino, R., Binaschi, M., Capolongo, L., Grandi, M., Suarato, A., and Zunino, F. (1994) Influence of structural modifications at the 3′ and 4′ positions of doxorubicin on the drug ability to trap topoisomerase II and to overcome multidrug resistance. *Mol. Pharmacol. 45*, 908–915.
13. Zhu, L., Cao, X., Chen, W., Zhang, G., Sun, D., and Wang, P. G. (2005) Syntheses and biological activities of daunorubicin analogs with uncommon sugars. *Bioorg. Med. Chem. 13*, 6381–6387.
14. Timmons, S. C., and Thorson, J. S. (2008) Increasing carbohydrate diversity via amine oxidation: aminosugar, hydroxyaminosugar, nitrososugar, and nitrosugar biosynthesis in bacteria. *Curr. Opin. Chem. Biol. 12*, 297–305.
15. Zhang, H., White-Phillip, J. A., Melancon, C. E., 3rd, Kwon, H. J., Yu, W. L., and Liu, H. W. (2007) Elucidation of the kijanimicin gene cluster: insights into the biosynthesis of spirotetronate antibiotics and nitrosugars. *J. Am. Chem. Soc. 129*, 14670–14683.
16. Kim, C. G., Lamichhane, J., Song, K. I., Nguyen, V. D., Kim, D. H., Jeong, T. S., Kang, S. H., Kim, K. W., Maharjan, J., Hong, Y. S., Kang, J. S., Yoo, J. C., Lee, J. J., Oh, T. J., Liou, K., and Sohng, J. K. (2008) Biosynthesis of rubradirin as an ansamycin antibiotic from Streptomyces achromogenes var. rubradiris NRRL3061. *Arch. Microbiol. 189*, 463–473.
17. Hosted, T. J., Wang, T. X., Alexander, D. C., and Horan, A. C. (2001) Characterization of the biosynthetic gene cluster for the oligosaccharide antibiotic, Evernimicin, in *Micromonospora carbonacea var. africana* ATCC39149. *J. Ind. Microbiol. Biotechnol. 27*, 386–392.
18. Fang, J., Zhang, Y., Huang, L., Jia, X., Zhang, Q., Zhang, X., Tang, G., and Liu, W. (2008) Cloning and characterization of the tetrocarcin A gene cluster from *Micromonospora chalcea* NRRL 11289 reveals a highly conserved strategy for tetronate biosynthesis in spirotetronate antibiotics. *J. Bacteriol. 190*, 6014–6025.
19. Hu, Y., Al-Mestarihi, A., Grimes, C. L., Kahne, D., and Bachmann, B. O. (2008) A unifying nitrososynthase involved in nitrosugar biosynthesis. *J. Am. Chem. Soc. 130*, 15756–15757.
20. Thorpe, C., and Kim, J. J. (1995) Structure and mechanism of action of the acyl-CoA dehydrogenases. *FASEB J. 9*, 718–725.
21. Kim, J. J., and Miura, R. (2004) Acyl-CoA dehydrogenases and acyl-CoA oxidases. Structural basis for mechanistic similarities and differences. *Eur. J. Biochem. 271*, 483–493.
22. Thoden, J. B., Timson, D. J., Reece, R. J., and Holden, H. M. (2005) Molecular structure of human galactokinase: implications for Type II galactosemia. *J. Biol. Chem. 280*, 9662–9670.
23. Terwilliger, T. C., and Berendzen, J. (1999) Automated MAD and MIR structure solution. *Acta Crystallogr. D Biol. Crystallogr. 55* (Pt 4), 849–861.
24. Terwilliger, T. C. (2000) Maximum-likelihood density modification. *Acta Crystallogr. D Biol. Crystallogr. 56* (Pt 8), 965–972.
25. Terwilliger, T. C. (2003) Automated main-chain model building by template matching and iterative fragment extension. *Acta Crystallogr. D Biol. Crystallogr. 59*, 38–44.
26. Emsley, P., and Cowtan, K. (2004) Coot: model-building tools for molecular graphics. *Acta Crystallogr. D Biol. Crystallogr. 60*, 2126–2132.
27. McCoy, A. J., Grosse-Kunstleve, R. W., Adams, P. D., Winn, M. D., Storoni, L. C., and Read, R. J. (2007) Phaser crystallographic software. *J. Appl. Crystallogr. 40*, 658–674.
28. Murshudov, G. N., Vagin, A. A., and Dodson, E. J. (1997) Refinement of macromolecular structures by the maximum-likelihood method. *Acta Crystallogr. D Biol. Crystallogr. 53*, 240–255.
29. Bannister, B., and Zapotocky, B. A. (1992) Protorubradirin, an antibiotic containing a C-nitroso-sugar fragment, is the true secondary metabolite produced by *Streptomyces achromogenes* var. rubradiris. Rubradirin, described earlier, is its photo-oxidation product. *J. Antibiot.* (*Tokyo*) *45*, 1313–1324.
30. Krissinel, E., and Henrick, K. (2004) Secondary-structure matching (SSM), a new tool for fast protein structure alignment in three dimensions. *Acta Crystallogr. D Biol. Crystallogr. 60*, 2256–2268.
31. Battaile, K. P., Nguyen, T. V., Vockley, J., and Kim, J. J. (2004) Structures of isobutyryl-CoA dehydrogenase and enzyme-product complex: comparison with isovaleryl- and short-chain acyl-CoA dehydrogenases. *J. Biol. Chem. 279*, 16526–16534.
32. Laskowski, R. A., Moss, D. S., and Thornton, J. M. (1993) Main-chain bond lengths and bond angles in protein structures. *J. Mol. Biol. 231*, 1049–1067.
33. DeLano, W. L. (2002) The PyMOL Molecular Graphics System. DeLano Scientific, San Carlos, CA, USA, The PyMOL Molecular Graphics System.